

# RSC Advances



This is an *Accepted Manuscript*, which has been through the Royal Society of Chemistry peer review process and has been accepted for publication.

*Accepted Manuscripts* are published online shortly after acceptance, before technical editing, formatting and proof reading. Using this free service, authors can make their results available to the community, in citable form, before we publish the edited article. This *Accepted Manuscript* will be replaced by the edited, formatted and paginated article as soon as this is available.

You can find more information about *Accepted Manuscripts* in the [Information for Authors](#).

Please note that technical editing may introduce minor changes to the text and/or graphics, which may alter content. The journal's standard [Terms & Conditions](#) and the [Ethical guidelines](#) still apply. In no event shall the Royal Society of Chemistry be held responsible for any errors or omissions in this *Accepted Manuscript* or any consequences arising from the use of any information it contains.

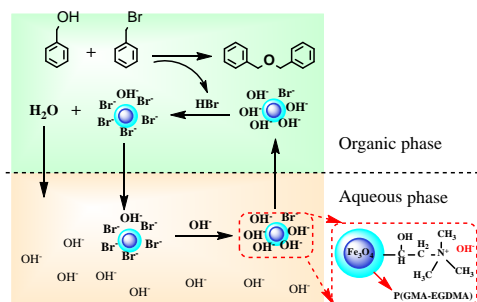
**Responses to Editor:**

1. A table of contents entry. This should include:

\* *Colour graphic: maximum size 8 cm x 4 cm*

\* *Text: one sentence, of maximum 20 words, highlighting the novelty of the work.*

Answer:



We have revealed a high efficiency, high dispersibility, structural stability, easy recovery and reusable magnetic phase transfer catalyst.

## Quaternary ammonium functionalized Fe<sub>3</sub>O<sub>4</sub>@P(GMA-EGDMA) composite particles as high efficiency and dispersibility catalysts for phase transfer reaction

Received 00th January 20xx,  
Accepted 00th January 20xx

DOI: 10.1039/x0xx00000x

www.rsc.org/

Xiangkun Jia<sup>a</sup>, Xinlong Fan<sup>a</sup>, Yin Liu<sup>a</sup>, Wei Li<sup>a</sup>, Lei Tian<sup>a</sup>, Lili Fan<sup>a</sup>, Baoliang Zhang<sup>a</sup>, Hepeng Zhang<sup>a</sup> and Qiuyu Zhang\*<sup>a</sup>

This work describes the synthesis and catalysis behavior of magnetic nanoparticles supported quaternary ammonium phase transfer catalysts Fe<sub>3</sub>O<sub>4</sub>@P(GMA-EGDMA)N<sup>+</sup>(CH<sub>3</sub>)<sub>3</sub>OH<sup>-</sup> (MQPTCs). The MQPTCs prepared by compositing P(GMA-EGDMA) on Fe<sub>3</sub>O<sub>4</sub> magnetic nanoparticle via seeded emulsion polymerization and quaternized by trimethylamine were characterized by SEM, TEM, FTIR, TGA and VSM, and core-shell structured MQPTCs with an exchange capacity of 1.14 mmol/g were obtained. Catalytic activity of the MQPTCs was evaluated via the investigation of efficiency of the conversion of benzyl alcohol and benzyl bromide into dibenzyl ether. In addition, the influences of the concentrations of catalysts and species of catalysts (different exchange capacities of MQPTCs) on conversion were studied in detail. The results demonstrated that the MQPTCs showed high efficiency with a conversion of 95% in only 6 h that was comparable with small molecule PTCs, and excellent reusability with a conversion of 94.1% after reused for 8 times.

### 1. Introduction

Over the past several decades, the investigation of phase transfer catalysts (PTCs) has attracted much attention owing to their effective utility in organic synthesis[1-8]. The major function of PTCs is to extract ionic reactant out of one phase and into the other phase where the reaction can take place, as a result of which the concentration of reactant in reaction phase is increased, thus accelerating the rate of multiphase reaction and improving the reaction efficiency[9]. However, the use of soluble small molecule PTCs in plenty of organic synthesis reactions is generally inapplicable for the prime reason that they are difficult to be removed from the reaction system at the end of the reaction, which leads to the reduction of the purity and property of the products[3]. Using non-recyclable small molecule PTCs is unacceptable in terms of economy[10] under some circumstances, and causes eutrophication of water if they were discharged into the environment because of nitrogen and phosphorus in PTCs[11-13]. Fortunately, these problems can be improved when polymer-supported PTCs emerged in recent years which were prepared via loading active-sites chemically on polymer supporters[7, 10, 14, 15]. As the properties and structure of active components on polymer-supported PTCs are identical with non-supported soluble small molecule PTCs, the polymer-supported PTCs not only inherit the high-efficiency of common PTCs, but also can be removed from the system after reaction. The preponderant feature of the polymer-supported PTCs is

embodied in the high reusability, accordingly, the cost of the organic synthesis is controllable.

Although the polymer-supported PTCs are recyclable after the reaction, the separation process remains unsatisfactory. The existing methods to remove polymer-supported PTCs from reaction mixture including filtration, natural sedimentation and centrifugation are time-consuming and energy-intensive processes. While in the past few decades, magnetic nanoparticles have been introduced to composite with functional materials to enhance their separation process on account of the readily separability and recoverability by external magnetic field[15-21]. Kawamura et al.[22] prepared the first example of magnetic nanoparticles-supported PTCs through the immobilization of small molecule quaternary ammonium and phosphonium salts on magnetic nanoparticles which were obtained by conventional coprecipitation method[23], they reported that the catalysts could be removed easily using an external magnet and were reusable for four times without significant loss of their catalytic reactivity by using 3 mol% catalyst based on reactant. However, the magnetic nanoparticles loaded an unacceptable low capacity of quaternary ammonium and phosphonium groups ranging from 0.10 to 0.25 mmol/g. Moreover, the magnetic nanoparticles-supported PTCs are difficult to avoid agglomerating due to their tiny size. The capacity and the dispersibility were crucial for supported catalysts. The dosage of catalysts could be decreased when the catalysts had more effective constituents. High dispersibility guaranteed the uniform of reaction processes, and further decreased the amount of catalysts, accelerated the rate of reaction.

<sup>a</sup> Department of Applied Chemistry, School of Science, Northwestern Polytechnical University, No. 127, West Youyi Road, Xi'an 710072, Shaanxi, China.

Eventually, the cost of production could be reduced. Therefore, it is necessary to pay much attention to increase the capacity of active-sites on the magnetic nanoparticles-supported PTCs and improve their dispersibility so as to make use of them to economically prepare productions on an industrial scale.

Herein, we carried out studies in an effort to enhance the dispersibility and increase the capacity of active-sites on magnetic nanoparticles-supported PTCs which were prepared by compositing and quaternizing of poly(glycidyl methacrylate-ethyleneglycol dimethacrylate (P(GMA-EGDMA)) on Fe<sub>3</sub>O<sub>4</sub> nanoparticle surfaces. Since GMA was general reaction scaffold due to the high activity and easy post-modification, the introduction of GMA could not only improve the dispersibility of composite nanoparticles but also bring the functional groups to increase the exchange capacity and further enhance the catalytic efficiency of magnetic nanoparticles-supported PTCs composite microspheres. The ability of the separation of PTCs composite microspheres could be greatly raised by external magnet at the end of reaction, which was attributed to the high magnetic responsibility of Fe<sub>3</sub>O<sub>4</sub> nanoparticles prepared by solvothermal method. The catalytic activity of this magnetic nanoparticles-supported PTCs was investigated through catalyzing the nucleophilic reaction between benzyl alcohol and benzyl bromide.

## 2. Experimental

### 2.1 Materials

Glycidyl methacrylate (GMA, 95%, Sartomer Company) and ethyleneglycol dimethacrylate (EGDMA, 98%, J&K Scientific, Ltd.) were purified to remove inhibitor by passing through alkaline Al<sub>2</sub>O<sub>3</sub> column and stored in a refrigerator prior to use. 2,2'-Azobis(2-methylpropionamide) dihydrochloride (V-50), hexadecyl trimethyl ammonium bromide (CTAB),  $\gamma$ -(methacryloyloxy)propyltrimethoxysilane (MPS), trimethylamine (TMA), 1,4-dioxane, benzyl alcohol, benzyl bromide, toluene, ethanol, sodium hydroxide (NaOH) and tetrabutyl ammonium bromide (TBAB) were procured from commercial sources and used as received. Methanol (HPLC grade) was purchased from J & K Scientific Ltd. Deionized water was used throughout the whole experiment. Fe<sub>3</sub>O<sub>4</sub> nanoparticles were prepared according to the procedure reported in the early literature of our research group[17].

### 2.2 Synthesis of Fe<sub>3</sub>O<sub>4</sub>@P(GMA-EGDMA) composite particles

Fe<sub>3</sub>O<sub>4</sub> nanoparticles prepared in advance were modified with double bond by grafting MPS in ethanol[24]. GMA as functional monomer and EGDMA as crosslinker were employed to produce Fe<sub>3</sub>O<sub>4</sub>@P(GMA-EGDMA) composite particles via a modified seeded emulsion polymerization technique[25]. The detailed experimental conditions in this paper are listed in Table S1. Typically, MPS modified Fe<sub>3</sub>O<sub>4</sub> particles (0.05g) dispersed in ethanol (8mL) by ultrasonic were added into a three-neck round-bottomed flask equipped with a paddle agitator and a reflux condenser, then GMA and EGDMA emulsified in aqueous solution of CTAB (0.02g in 50 mL water) by ultrasonic were added into the mixture. 0.02 g V-50 dissolved in 10 mL water was added into the emulsion to start the polymerization when the temperature was increased to 75 °C. After

stirring at 200 rpm for 12 h, the Fe<sub>3</sub>O<sub>4</sub>@P(GMA-EGDMA) composite particles were obtained by separating in the present of magnet and washing with water and ethanol for 5 times. Finally, the separated product was freeze-dried. The percentage of P(GMA-EGDMA) on the composite particles could be obtained by TG.

### 2.3 Preparation of magnetic nanoparticles-supported quaternary ammonium phase transfer catalysts

Through the TG data, we could gain the contents of P(GMA-EGDMA) on the composite particles, and then the molar weight of epoxy group would be estimated. Fe<sub>3</sub>O<sub>4</sub>@P(GMA-EGDMA) composite particles with different thicknesses of P(GMA-EGDMA) (0.1 g in 25 mL water) and TMA (approximately excessive 60 molar times of epoxy group, dispersed in 125 mL 1,4-dioxane) were blended into a three-neck round-bottomed flask at 200 rpm and heated to 60 °C. After stirring for 12 h, magnetic nanoparticles-supported quaternary ammonium phase transfer catalysts (MQPTCs) were obtained by separating in the present of magnet and washing with water and ethanol for 5 times, then freeze-dried. The MQPTCs were sealed and stored at room temperature.

### 2.4 Evaluation of the catalytic activity of MQPTCs

The oil phase contained benzyl alcohol (0.81 g, 7.5 mmol), benzyl bromide (1.28 g, 7.5 mmol) and toluene (13.05 g) was added into a three-neck round-bottomed flask equipped with a paddle agitator and reflux condenser, then aqueous phase consisted of MQPTCs ultrasonically dispersed into a mixture of H<sub>2</sub>O (15 g) and NaOH (15 g) was added into the oil phase. The phase transfer reaction was carried out at a stirring rate of 400 rpm and a temperature of 40°C. In order to evaluate the catalytic activity of MQPTCs, oil samples taken at time intervals were used for determining the conversion rate of the phase transfer reaction. 0.1 g oil phase (accurate to 0.1 mg) was dissolved in 20 mL methanol, then diluted to 100 mL for measurement by high performance liquid chromatography (HPLC). The ultimate yield was confirmed by HPLC with the flowing phase composed of methanol and water (v:v=80:20). The yields ( $y$ ) of this phase transfer catalytic reaction were calculated by the following formulae:

$$y = (\omega \times W) / [(\omega \times M_{\text{HBr}} + M_{\text{dibenzyl ether}}) \times m] \quad (1)$$

$$W = w_1 + w_2 + w_3 \quad (2)$$

$$\omega = (A \times 10^{-7} \times 5.0006 + 0.0002) / M \quad (3)$$

$w_1$ ,  $w_2$  and  $w_3$  were the weight of benzyl alcohol, benzyl bromide and toluene added into the reaction system, respectively.  $M$  was the less mole between benzyl alcohol and benzyl bromide added into the reaction system.  $M_{\text{HBr}}=80.904$  g/mol,  $M_{\text{dibenzyl ether}}=198.26$  g/mol.  $\omega$  was the mass fraction of dibenzyl ether produced in oil phase. The formula was matched by a series of data points of mass fraction versus the integral area of dibenzyl ether which were measured by HPLC (Fig. S1).  $M$  was the accurate weight of sample

of oil phase. **A** was the integral area of dibenzyl ether measured by HPLC.

After phase transfer catalytic reaction, the MQPTCs were separated from the system by an external magnetic field, washed with water and ethanol for 5 times, and then freeze-dried for next use.

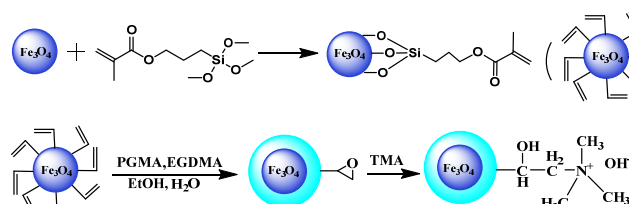
## 2.5 Characterization

The P(GMA-EGDMA) contents on the magnetic composite particle surfaces were measured by thermogravimetric analysis (TGA) on a Q50 (TA Instruments) with a temperature from room temperature to 800 °C and a heating rate of 10 °C/min. Fourier transform infrared spectra (FTIR) were performed on a TENSOR27 FTIR spectrometer (Bruker). The morphologies of composite particles were observed by scanning electron microscopy (SEM, JSM-6700F, JEOL, Japan), samples dispersed in ethanol were dropped onto silicon wafers and then sputtered with platinum by a JFC-1600 auto fine coater at a current of 20 mA for 180 s before examination. Transmission electron microscopy (TEM, JEM-3010, JEOL, Japan) was operated at an accelerating voltage of 200 kV. The samples for TEM observations were prepared by depositing particles on copper grids, and evaporating the water at room temperature before measurement. The magnetic properties of magnetic nanoparticles were evaluated by a vibrating sample magnetometer (VSM, VersaLab, Quantum Design, USA). HPLC from Hitachi was used to measure the yield of the phase transfer catalytic reaction with the flowing phase composed of methanol and water (v:v=80:20).

## 3. Results and Discussion

### 3.1 Synthesis and Structure of Fe<sub>3</sub>O<sub>4</sub>@P(GMA-EGDMA) and MQPTCs composite particles

The preparation procedure of MQPTCs was exhibited in Scheme 1, Fe<sub>3</sub>O<sub>4</sub> particles were modified by MPS, then coated with P(GMA-EGDMA) via a seeded emulsion polymerization, finally, the MQPTCs were produced after quaternized by TMA. Typical structures of Fe<sub>3</sub>O<sub>4</sub>, MPS modified Fe<sub>3</sub>O<sub>4</sub> and Fe<sub>3</sub>O<sub>4</sub>@P(GMA-EGDMA) with different amounts of P(GMA-EGDMA) particles are characterized by TEM and SEM, and shown in Fig. 1. Image in Fig. 1a shows that many primary crystals aggregated and assembled to form Fe<sub>3</sub>O<sub>4</sub> nanoparticles with rough surfaces. The surface morphologies and particle sizes of the magnetic nanoparticles had no obvious change when MPS was introduced (Fig. 1b). While obvious smooth surface was obtained once P(GMA-EGDMA) was coated on the Fe<sub>3</sub>O<sub>4</sub> surface. From the TEM images, it could be found that the thickness of P(GMA-EGDMA) around the core particles was increased along with the increasing of the amounts of GMA and EGDMA in the emulsion system (Fig. 1c-f). When the percentage of P(GMA-EGDMA) was up to 50.8%, some small protuberances formed by polymers were attached to the magnetic composite particles, leading to unsmooth surfaces (Fig. 1g), which was possibly because that P(GMA-EGDMA) nanoparticles formed by the emulsion polymerization of radical decomposed in water were captured by the magnetic composite particles. Fig. 1h presents the morphology of MQPTCs with 44.6% P(GMA-EGDMA), it could be found that the surface of MQPTCs had no change comparing with corresponding Fe<sub>3</sub>O<sub>4</sub>@P(GMA-EGDMA) composite particles.



Scheme 1. Schematic illustration of the preparation of MQPTCs.

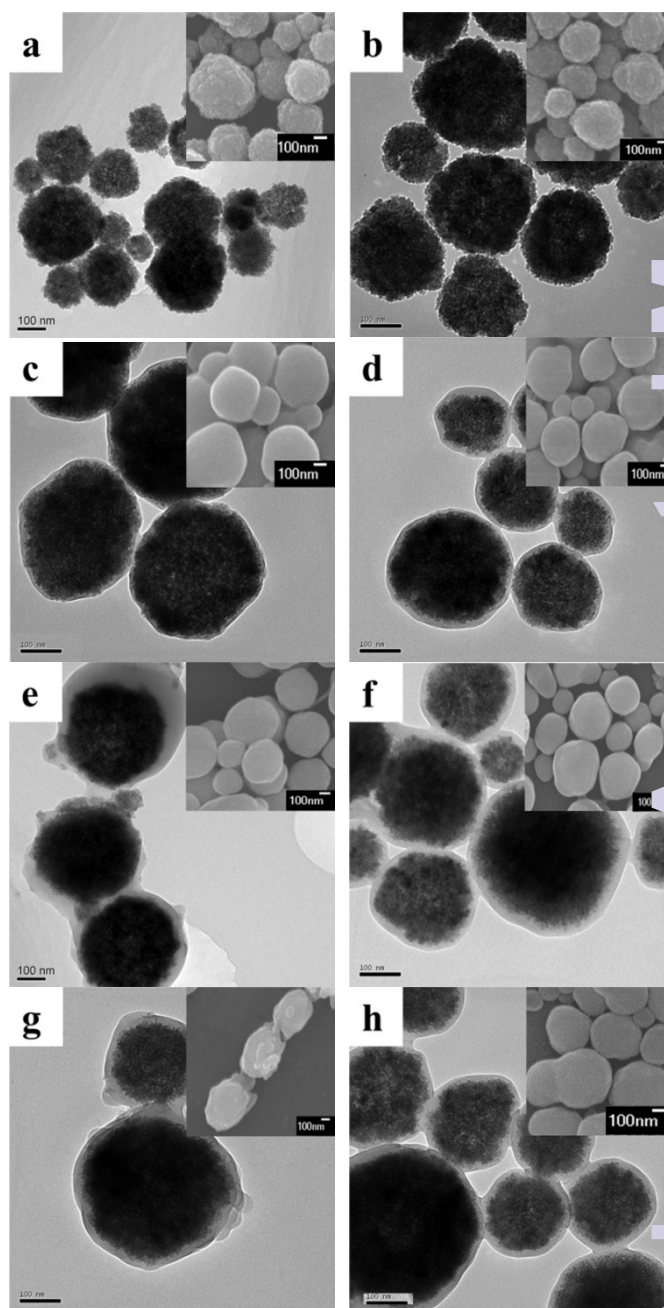


Fig. 1. TEM and SEM images of Fe<sub>3</sub>O<sub>4</sub> nanoparticles (a); Fe<sub>3</sub>O<sub>4</sub> modified by MPS (b); Fe<sub>3</sub>O<sub>4</sub>@P(GMA-EGDMA) composite particles with different percentages of P(GMA-EGDMA): 19.9%(c); 30.4%(d); 35.9%(e); 44.6%(f); 50.8%(g) and MQPTCs with 44.6% P(GMA-EGDMA)(h).

Fig. 2 shows TGA curves of Fe<sub>3</sub>O<sub>4</sub> nanoparticles, MPS modified Fe<sub>3</sub>O<sub>4</sub> and Fe<sub>3</sub>O<sub>4</sub>@P(GMA-EGDMA) with different amounts of P(GMA-EGDMA). The DTA curves of Fe<sub>3</sub>O<sub>4</sub> and Fe<sub>3</sub>O<sub>4</sub>@P(GMA-

EGDMA) were displayed at Fig. S2. It was obvious that there was a small weight loss from initial temperature to about 280 °C, which could be attributed to the evaporation of water and residual organic solvent. From 280 °C to 550 °C, the tiny weight loss of Fe<sub>3</sub>O<sub>4</sub> nanoparticles was due to the decomposition of small molecules such as sodium acetate absorbed during the preparation process (Fig. 2a). MPS modified Fe<sub>3</sub>O<sub>4</sub> had more weight loss than Fe<sub>3</sub>O<sub>4</sub> nanoparticles because of the silane coupling agent attached (Fig. 2b), and the magnetic contents of curve b is about 93.4%. When the amounts of GMA were increased during the seeded emulsion polymerization, the magnetic contents of Fe<sub>3</sub>O<sub>4</sub>@P(GMA-EGDMA) composite particles were decreased to 74.8%, 65.0%, 59.9%, 51.8% and 46.0% (Fig. 2c-g), respectively. And the percentage of P(GMA-EGDMA) on the composite particles could be calculated by the following formula:

$$\xi = (\eta_1 - \eta_2) / \eta_1 \times 100\% \quad (4)$$

$\eta_1$  and  $\eta_2$  were the percentage of inorganic component of Fe<sub>3</sub>O<sub>4</sub> modified by MPS and Fe<sub>3</sub>O<sub>4</sub>@P(GMA-EGDMA) with different thicknesses of P(GMA-EGDMA), respectively. The percentages of P(GMA-EGDMA) on the composite particles were 19.9%, 30.4%, 35.9%, 44.6% and 50.8%, respectively.

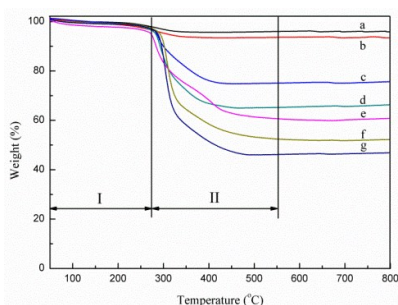


Fig. 2. TGA curves of Fe<sub>3</sub>O<sub>4</sub> nanoparticles(a), Fe<sub>3</sub>O<sub>4</sub> modified by MPS(b) and Fe<sub>3</sub>O<sub>4</sub>@P(GMA-EGDMA) with different amounts of P(GMA-EGDMA): 19.9%(c); 30.4%(d); 35.9%(e); 44.6%(f); 50.8%(g).

In order to further prove the successful coating of P(GMA-EGDMA) and quaternization of epoxy groups, FTIR was used to research the alteration of functional groups of the composite particles. Fig. 3 shows the FTIR spectra of Fe<sub>3</sub>O<sub>4</sub> nanoparticles (Fig. 3a), Fe<sub>3</sub>O<sub>4</sub> modified by MPS (Fig. 3b), Fe<sub>3</sub>O<sub>4</sub>@P(GMA-EGDMA) composite particles (Fig. 3c) and quaternized magnetic composite particles (Fig. 3d). It is quite clear that the strong peak at 579 cm<sup>-1</sup> corresponded to the characteristic of Fe-O vibration. The adsorption peaks at 1186 and 960 cm<sup>-1</sup> could be attributed to the stretching vibration of C-C and Si-O of MPS attached to Fe<sub>3</sub>O<sub>4</sub> particles, respectively (Fig. 3b). In curve c, the distinct C=O and C-H stretching vibrations at 1724 and 2941 cm<sup>-1</sup> proved the successful coating of P(GMA-EGDMA) on the magnetic particles. The peak at 1167 cm<sup>-1</sup> is the stretching vibrations of C-O-C of ester group. The existence of epoxy groups is confirmed by the peaks at 856 cm<sup>-1</sup> of ring stretching vibration. When the magnetic composite particles were quaternized, the strength of peaks at 856 cm<sup>-1</sup> was greatly weakened, and C-N adsorption peak appeared at 1562 cm<sup>-1</sup>. All the results proved that P(GMA-EGDMA) was successfully coated on the

surface of Fe<sub>3</sub>O<sub>4</sub> magnetic particles, and the epoxy group was successfully quaternized by TMA.

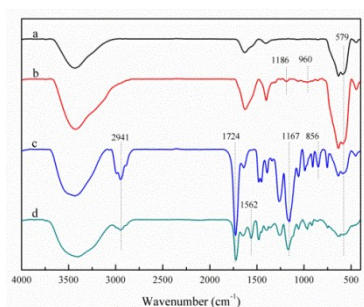


Fig. 3. FTIR spectra of Fe<sub>3</sub>O<sub>4</sub> nanoparticles(a), Fe<sub>3</sub>O<sub>4</sub> modified by MPS(b); Fe<sub>3</sub>O<sub>4</sub>@P(GMA-EGDMA) (c) and quaternized composite particles(d).

The magnetic responsivity of the magnetic particles which is usually evaluated by specific saturation magnetization is an important property for practical application. Fig. 4 presents the hysteresis loops of Fe<sub>3</sub>O<sub>4</sub> nanoparticles (Fig. 4a), MPS modified Fe<sub>3</sub>O<sub>4</sub> particles (Fig. 4b) and Fe<sub>3</sub>O<sub>4</sub>@P(GMA-EGDMA) with different amounts of P(GMA-EGDMA) (Fig. 4c-f). Apparently, the coercivity of all samples is almost negligible, indicating that all of the magnetic particles prepared in this paper possess superparamagnetic property and could be easily separated by external field. The specific saturation magnetization of Fe<sub>3</sub>O<sub>4</sub> particles was 62.6 emu/g, which proved that Fe<sub>3</sub>O<sub>4</sub> particles prepared by solvothermal method had an excellent magnetic responsivity and were easy to be manipulated by external magnetic field. When Fe<sub>3</sub>O<sub>4</sub> particles were modified by MPS, the specific saturation magnetization had a few decline (58.7 emu/g), probably because of the coating of silane coupling agent and mild oxidation under high temperature. Once coated by P(GMA-EGDMA), the specific saturation magnetization decreased along with the increasing of amounts of P(GMA-EGDMA). When the percentages of polymers on Fe<sub>3</sub>O<sub>4</sub>@P(GMA-EGDMA) composite particles were 19.9%, 30.4%, 35.9%, 44.6% and 50.8%, the specific saturation magnetizations of them were 49.7, 44.4, 41.6, 35.7 and 32.0 emu/g, respectively. The insert picture in Fig. 4 indicated that the MQPTCs dispersed in aqueous phase gathered together completely within 15s under an external magnetic field and redispersed quickly with a slight shake once the magnetic field was removed. There is a strong linear relationship between the percentages of inorganic component pure Fe<sub>3</sub>O<sub>4</sub> and the specific saturation magnetizations (Fig. S3), which proved that the specific saturation magnetizations of the composite particles decreased linearly as the increasing of polymer coating.

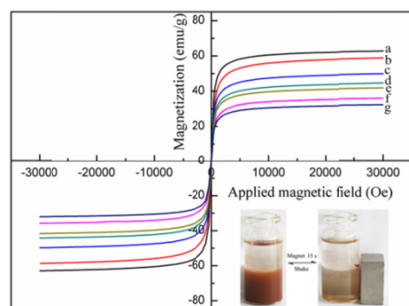


Fig. 4. The hysteresis loops of  $\text{Fe}_3\text{O}_4$  nanoparticles (a), MPS modified  $\text{Fe}_3\text{O}_4$  (b)  $\text{Fe}_3\text{O}_4@P(\text{GMA-EGDMA})$  with different percentages of P(GMA-EGDMA): 19.9%(c); 30.4%(d); 35.9%(e); 44.6%(f); 50.8%(g).

The exchange capacity measured by acid-base titration method of MQPTCs with different percentages of polymer are given in Fig. 5. When the percentages of polymers on  $\text{Fe}_3\text{O}_4@P(\text{GMA-EGDMA})$  composite particles were 19.9%, 30.4%, 35.9%, 44.6% and 50.8%, the exchange capacities of quaternary ammonium composite particles were 0.15, 0.48, 0.61, 0.99 and 1.14 mmol/g, respectively, which were much larger than the capacity of previous report[22]. While the data of exchange capacity measured by acid-base titration were still smaller than theoretical value of quaternized groups calculated from percentages of polymers, mostly because the polymer could not be quaternized completely by TMA.

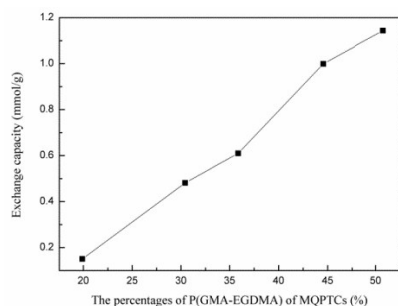
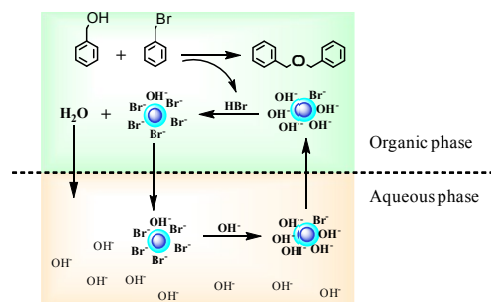


Fig. 5. The exchange capacity of MQPTCs with different percentages of P(GMA-EGDMA)

### 3.2 Evaluation of the catalytic activity of MQPTCs

In order to examine the catalytic activity of MQPTCs, the nucleophilic reaction between benzyl alcohol and benzyl bromide with removing HBr and producing dibenzyl ether in alkaline environment was chosen as model reaction (Scheme 2). Most of the MQPTCs dispersed in the aqueous phase or stayed at the interface between oil and aqueous phase and minor amount of the MQPTCs could enter into the oil phase because of the relatively stronger hydrophilicity and weaker hydrophobicity of the polymer. Three equilibriums including the distributions of MQPTCs, hydroxyl ions and bromide ions were created between the two phases. The  $\text{OH}^-$  carried by the MQPTCs entered into the oil combined with HBr produced by the nucleophilic reaction to generate  $\text{H}_2\text{O}$  and  $\text{Br}^-$ . As a result, the amount of  $\text{OH}^-$  in the oil phase was decreased, while the amount of  $\text{Br}^-$  in the oil phase was increased. The equilibriums of the distributions of  $\text{OH}^-$  and  $\text{Br}^-$  were broken, leading to the MQPTCs adsorbed  $\text{Br}^-$  in the oil phase transfer to aqueous phase

and the MQPTCs adsorbed  $\text{OH}^-$  in the aqueous phase transfer to oil phase. In the alkaline environment, abundant  $\text{OH}^-$  in aqueous phase replaced  $\text{Br}^-$  on the MQPTCs to regenerate the MQPTCs, then the MQPTCs turned into oil phase to catalyze the reaction again.



Scheme 2. Schematic illustration of the phase transfer reaction catalyzed by MQPTCs.

The effect of variation of exchange capacity of MQPTCs on the phase transfer catalytic reaction was investigated in the range of 0.15 to 1.14 mmol/g (Fig. 6). By controlling an equal mole of quaternary ammonium groups at 0.6 mol% of the reactant added into the reaction system. It was found that the exchange capacity of MQPTCs had little impact on the phase transfer catalytic system. No matter how low the exchange capacity was, the conversion could reach about 95% in only 6-8 h, and could be comparable to the small molecule catalyst TBAB. While the initial slope of TBAB was a little bigger than MQPTCs maybe because that TBAB could migrate in two phases quickly owing to their small sizes. The control experiments were consist of two sections, one was catalyzed by  $\text{Fe}_3\text{O}_4@P(\text{GMA-EGDMA})$  composite particles which was not quaternized by TMA, and the other was no PTCs added in the reaction. When the MQPTCs were replaced by  $\text{Fe}_3\text{O}_4@P(\text{GMA-EGDMA})$ , the conversion was 61.9% after 24 h because of the migration of HBr absorbed on organic-inorganic composite particles  $\text{Fe}_3\text{O}_4@P(\text{GMA-EGDMA})$  from oil phase to aqueous phase. While no PTCs were added, the conversion just was 38.3% after 24 h, thus the reaction rate was much lower obviously.

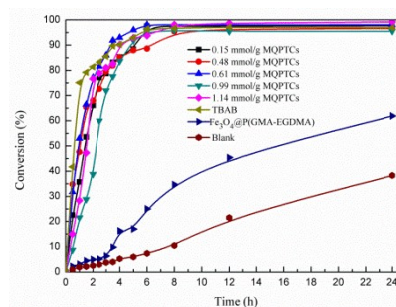


Fig. 6. The variation of conversion with the extended reaction time of different exchange capacities of MQPTCs, TBAB and without PTCs.

The MQPTCs in the range of 0.1 mol% to 2.0 mol% (based on the mole of reactant) of the catalyst with an exchange capacity of 0.9 mmol/g were used to study the effect of concentrations of catalysts on the rate of phase transfer catalytic reaction. From Fig. 7, it could

be seen that when the amounts of catalyst were increased, the reaction rate increased distinctly. Nevertheless when the amount of catalysts was increased to 2.0 mol%, the conversion rate curve was close to the case of 1.0 mol%, which was probably because of the saturation of catalysts. The conversion ratio could reach 96.8% when the reaction was catalyzed by 0.1 mol% MQPTCs for 24 h. By raising the amounts of catalysts to 0.2 mol%, the conversion ratio attained to 95.1% after 12 h and 97.4% after 24 h. When 0.6 mol% MQPTCs was added, the conversion ratio reached 95.4% in 6 h, and increased to 97.5% after 24 h. When the amounts of catalysts reached 1.0 mol%, the conversion ratio became 96.3% in only 3.5 h, and 98.8% in 24 h. By further increasing the MQPTCs to 2.0 mol%, 95.0% conversion ratio was achieved after 2.5 h, and after 24 h, the conversion ratio was increased to 98.4%. The efficiency of producing dibenzyl ether catalyzed by MQPTCs was much higher than previous reports[26, 27].

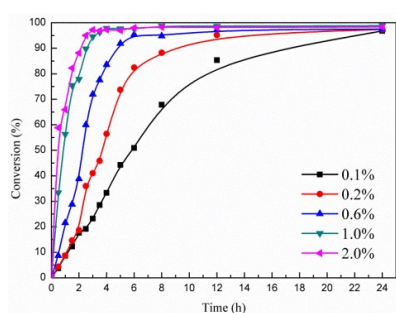


Fig. 7. The variation of conversion with the extended reaction time of different dosages of MQPTCs.

Separated easily and rapidly by external magnet is the most favorable feature of the magnetic particles-supported quaternary ammonium phase transfer catalysts. After the reaction, the MQPTCs were collected by using a magnet, and the catalysts stayed at the bottom of the reaction vessel was washed and dried to reuse directly. The recycle and reuse of the MQPTCs for the phase transfer catalytic reaction were examined at 40 °C for 24 h with 0.6 mol% MQPTCs. As presented in Fig. 8, the MQPTCs showed no significant loss of catalytic activity and reached a conversion ratio of 94.1% when they were reused for 8 times. The MQPTCs reused 8 times were characterized by TEM, SEM and FTIR (Fig. 9). From Fig. 9a, we could find that the morphologies of the used MQPTCs had no change comparing with the unused MQPTCs. The FTIR data (Fig. 9b) showed that the C-N adsorption peak at 1562  $\text{cm}^{-1}$  of used MQPTCs was still existed, and the important peak of hydroxyl was also strong enough, the structure was not broken after the phase transfer catalytic reaction. And the MQPTCs remained excellent dispersibility without any agglomeration even after 8 cycles (Fig. S4), which was much better than previous report[22].

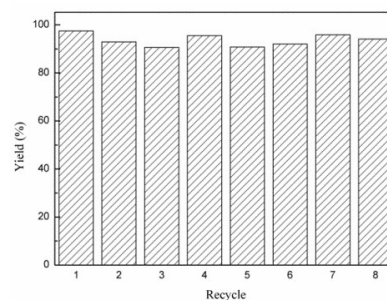


Fig. 8. Recycling of the MQPTCs for the preparation of dibenzyl ether.

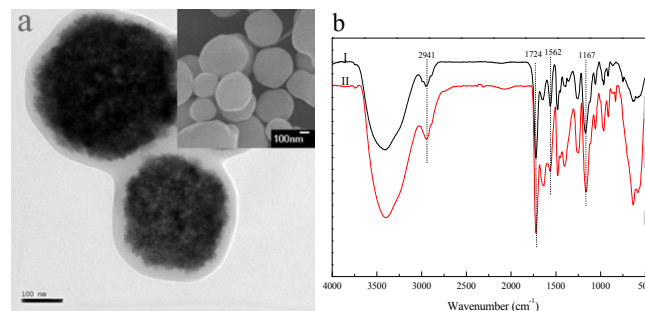


Fig. 9. (a)TEM and SEM image of MQPTCs after reused 8 times; (b)FTIR spectra of quaternized composite particles(I) and MQPTCs after reused 8 times(II).

## Conclusions

We have demonstrated the preparation and the efficiency on producing of dibenzyl ether by using magnetic particles-supported quaternary ammonium phase transfer catalysts in this paper. The results of the experiments indicated that the conversion of phase transfer reaction catalyzed by MQPTCs composite particles could reach to 95% in only 6 h, showing high efficiency comparing with small molecule PTCs. More importantly, the catalysts have a high exchange capacity of 1.14 mmol/g and could be recycled easily and rapidly via an external magnetic field. Moreover, the catalytic activity can be kept well after catalyzing the phase transfer reaction 8 times. Furthermore, the morphology and dispersibility of MQPTCs reused 8 times have no significant change comparing with the unused MQPTCs. To sum up, we have revealed a high efficiency, high dispersibility, structural stability, easy recovery and reusable catalyst which is expected to play an important role in economically preparation on an industrial scale.

## Acknowledgements

This work was supported by the National High Technology Research and Development Program of China (863 Program) (Grant No. 2012AA02A404), the Key Program of the National Natural Science Foundation of China (Grant No. 51433008), the General Program of the National Natural Science Foundation of China (Grant No. 51173146) and the Basic Research of Northwestern Polytechnical University (Grant No. 3102014JCQ01094, JC20120248, 3102014ZD).

**References**

- 1 K. Shanmugan, T. Balakrishnan, *Indian J. Chem. Sec. A*, 2007, 46A, 1069..
- 2 Y. Du, A. Liu, and L. He, *J.Org. Chem.*, 2008, 73, 4709.
- 3 E. Murugan, I. Pakrudheen, *Appl. Catal. A-General*, 2012, 439-440, 142.
- 4 U. Haldar, L. Ramakrishnan, K. Sivaprakasam, P. De, *Polymer*, 2014, 55, 5656.
- 5 E. Murugan, G. Tamizharasu, *J. Mol. Catal. A-Chem.*, 2012, 363-364, 81.
- 6 P. Vivekanand, T. Balakrishnan, *Catal. Commun.*, 2009, 10, 1371.
- 7 P. Vivekanand, T. Balakrishnan, *Catal. Commun.*, 2009, 10, 687.
- 8 P. Vivekanand, T. Balakrishnan, *Appl. Catal. A-General*, 2009, 364, 27.
- 9 M. Sharma, *Chem. Eng. Sci.*, 1988, 43, 1749.
- 10 E. Murugan, P. Gopinath, *Appl. Catal. A-General*, 2007, 319, 72.
- 11 S. Carpenter, N. Caraco, D. Correll, R. Howarth, A. Sharpley, V. Smith, *Ecol. Appl.*, 1998, 8, 559.
- 12 R. Jones, G. Lee, *Water Res.*, 1982, 16, 503.
- 13 J. Ryther, W. Dunstan, *Science*, 1971, 171, 1008.
- 14 S. Regen, *J. Am. Chem. Soc.*, 1975, 97, 5956.
- 15 A. Schatz, O. Reiser, W. Stark, *Chemistry*, 2010, 16, 8950.
- 16 B. Liu, D. Zhang, J. Wang, C. Chen, X. Yang, C. Li, *J. Phys. Chem. C*, 2013, 117, 6363.
- 17 M. Ma, Q. Zhang, D. Yin, J. Dou, H. Zhang, H. Xu, *Catal. Commun.*, 2012, 17, 168.
- 18 W. Li, B. Zhang, X. Li, H. Zhang, Q. Zhang, *Appl. Catal. A-General*, 2013, 459, 65.
- 19 Q. Yang, S. Ma, F. Lan, L. Xie, Y. Wu, B. He, Z. Gu, *Compos. Sci. Technol.*, 2014, 92, 34.
- 20 Z. Xiong, Y. Chen, L. Zhang, J. Ren, Q. Zhang, M. Ye, W. Zhang, H. Zou, *ACS Appl. Mater. Inter.*, 2014, 6, 22743.
- 21 W. Jiao, M. Shioya, R. Wang, F. Yang, L. Hao, Y. Niu, W. Liu, L. Zheng, F. Yuan, L. Wan, X. He, *Compos. Sci. Technol.*, 2014, 99, 124.
- 22 M. Kawamura, K. Sato, *Chem. Commun.*, 2006, 4718.
- 23 F. Guo, Q. Zhang, B. Zhang, H. Zhang, L. Zhang, *Polymer*, 2009, 50, 1887.
- 24 X. Li, B. Zhang, W. Li, X. Lei, X. Fan, L. Tian, H. Zhang, Q. Zhang, *Biosensors & bioelectronics*, 2014, 51, 261.
- 25 M. Pan, Y. Sun, J. Zheng, W. Yang, *ACS Appl. Mater. Inter.*, 2013, 5, 8351.
- 26 G. Joshi, S. Adimurthy, *Synthetic Commun.*, 2011, 41, 720.
- 27 H. rao, S. Senthilkumar, *Indian Acad. Sci.*, 2001, 113, 191.